Data Assimilation and Regional Forecasts Using Atmospheric InfraRed Sounder (AIRS) Profiles

Shih-Hung Chou*, Bradley Zavodsky†, Gary Jedlovec*

*NASA/Marshall Space Flight Center, Huntsville, AL
†Earth Science System Center, University of Alabama in Huntsville, Huntsville, AL

1. INTRODUCTION

One of the challenges in numerical weather prediction is to provide forecast models with an initial state that realistically describes the atmosphere. Observations from satellites are one valuable option to improve the model initial state, especially in data sparse regions. NASA's most state-of-the-art atmospheric profiler is the Atmospheric InfraRed Sounder (AIRS). AIRS radiances have been assimilated into global models yielding improvements in 500 hPa anomaly correlations out to 5-day forecasts (e.g. Le Marshall et al. 2006). However, for centers focusing on regional forecasting problems—such as NASA's SPoRT Center (Goodman et al. 2004)—AIRS profile impact on thermodynamic structures is a logical first step to using AIRS data. A methodology for assimilating AIRS profiles into the Weather Research and Forecasting (WRF) model using the three-dimensional variational (3DVAR) assimilation component of WRF (WRF-Var) is presented herein along with some preliminary forecast impact statistics from a 37-day case study period (17 January to 22 February 2007).

2. AIRS PROFILES

AIRS—coupled with the Advanced Microwave Sounding Unit (AMSU)—forms an integrated temperature and humidity sounding system. Due to its hyperspectral nature, AIRS can provide near-radiosonde-quality atmospheric temperature and moisture profiles with the ability to resolve some small-scale vertical features in both clear and partly cloudy scenes. AIRS has an instrument accuracy of 1K in 1km layers for temperature and 15% in 2km layers for relative humidity. The spatial resolution of the profiles at nadir is approximately 50 km (Aumann et al. 2003). The superior vertical resolution and sounding accuracy make the instrument very appealing as a complement to radiosonde measurements in data sparse regions. For this study, standard version 5.0 soundings that contain 14 vertical levels between 1000 and 50 hPa are used.

Each profile contains level-specific quality indicators (QIs) that define a specific level below which data are of questionable quality. This level is generally consistent with clouds and land effects (Susskind et al. 2006). In this study, the QIs are used to select the optimal data from each profile for assimilation. A three-dimensional distribution of AIRS profiles as determined by the QIs for 17 January 2007 is shown in Figure 1.

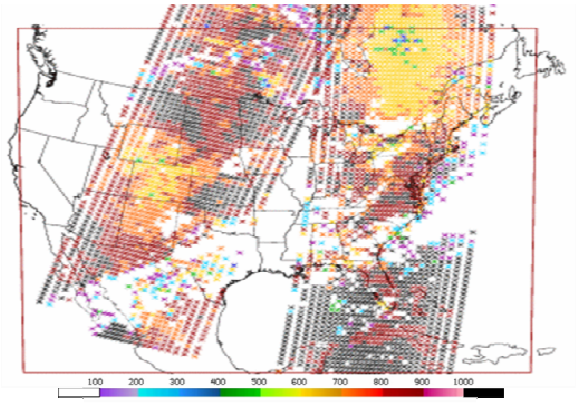

Fig. 1. Quality indicators for AIRS profiles assimilated at 0800 UTC on 17 January 2007. The black points represent the highest quality data, and each colored point denotes the pressure level above which there are quality data. The red rectangle denotes the bounds of the WRF model domain.

Poorly-defined infrared emissivity due to inhomogeneous land type can lead to degraded AIRS observations in over land soundings (Borbas 2007). Thus, over land observations generally have larger errors than those over water. In this study, both land and water soundings are assimilated and treated as two separate observation types in the analysis process. To accomplish this task, the WRF-Var source code was altered to accommodate AIRS-land and AIRS-water data sets with separate observation errors for the different observation types. Here, only the diagonal terms in the observation error matrix are filled. There are two strategies for assigning errors to observations from a satellite: 1) use the instrument accuracy or 2) use the validation of the instrument with dedicated in-situ

observations. Tobin et al. (2006) validated the AIRS thermodynamic profiles against dedicated sondes in the Southern Great Plains (SGP; for land soundings) and the Tropical Western Pacific (TWP; for water soundings). Since the SPoRT WRF domain is mid-latitudinal, validation using SGP sondes is applicable for the land retrievals; thus, land soundings are defined using the Tobin et al. (2006) estimates. On the other hand, the TWP does not represent the over-water environment within the mid-latitudinal domain, so the AIRS instrument specifications are instead used for these soundings. Additionally, this arrangement allows the over-water soundings to have slightly lower error than the over-land soundings, which is consistent with AIRS sounding characteristics. Figure 2 shows the observational errors for land (green line) and water (blue line) soundings (black line denotes background error; see section 3.3).

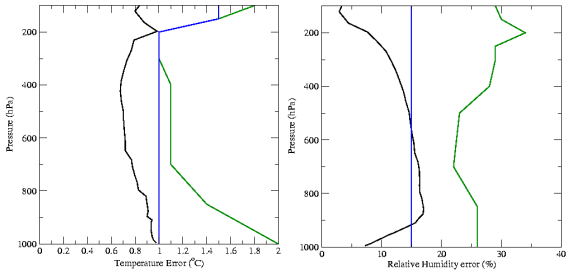

Fig. 2. Background (black) errors and observation (blue: AIRS-water, green: AIRS-land) errors for WRF-Var analysis for temperature (left) and relative humidity (right).

3. EXPERIMENTAL DESIGN

3.1. WRF Model Set-Up

The forecast model used herein is the Weather Research and Forecasting (WRF; Skamarock, 2005) model, a next-generation mesoscale numerical weather prediction system designed to serve both operational forecasting and atmospheric research needs. It is a limited-area, non-hydrostatic primitive equation model with multiple physical parameterization options. The model domain used herein consists of a 450 x 360 grid with 12-km spacing that covers the contiguous United States, Western Atlantic Ocean, and Gulf of Mexico (see Fig. 1). It has 37 staggered terrain-following vertical levels with the top-level pressure at 50 hPa and finest resolution near the lower boundary.

The WRF physical options used in this study consist of the Ferrier (new Eta) microphysics, the Kain-Fritsch cumulus convection scheme (Kain and Fritsch 1990), and the Mellor-Yamada-Janjic planetary boundary scheme (Mellor and Yamada 1982, Janjic 1990). The rapid radiative transfer model (RRTM, Mlawer et al 1997) and Dudhia scheme (Dudhia 1989) are used for longwave and shortwave radiation, respectively. The four-layer Noah land surface model (Chen and Dudhia 2001) provides the land surface physics.

For this case study, each day's WRF forecast is a cold start initialized using the 0000 UTC North American Mesoscale (NAM) analyses. The boundary conditions are updated every 3 hours using the NAM forecasts. Although a NAM analysis is available at 0600 UTC, using the 0000 UTC NAM as initial conditions allows the model to adjust dynamically prior to data assimilation. The WRF model is run from the initialization time to the time of the observations. This short-term WRF forecast is then used as the first guess field for the WRF-Var analysis. Because AIRS is a polar-orbiting satellite, the observation time for the AM overpass varies between 0600 and 0900 UTC. The assimilation time is determined by the mean time of 2 AIRS data swaths over central and eastern North America (the westernmost overpass is omitted as these data will likely have minimal impact on short-term forecasts over the eastern U.S. at 48 hours). The WRF-Var analysis, then, re-initializes the WRF for the AIRS-assimilated runs (AIRS) and produces a 48-h forecast. A control run (CNTL) is performed in the same manner except no data are assimilated.

3.2. WRF-Var Implementation

The WRF-Var is the data assimilation component of WRF (Barker et al., 2004), which works by minimizing a cost function to estimate the true state of the atmosphere using a previous forecast (background), observations, and their respective errors. These errors define the weighting at each grid point of the background and observations such that larger background error for a given variable will result in an analysis more closely resembling the observation (and vice versa). The observations are spread horizontally using a background error correlation length scale (Fig. 3), which is a function of grid point separation. The observations are spread vertically using an empirical orthogonal function (EOF) composition of the vertical component of the background error (Fig. 4).

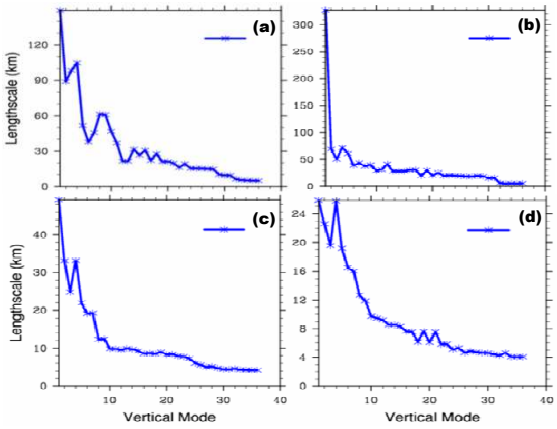

Fig. 3. Length scale for each control variable—a) streamfunction, b) velocity potential, c) temperature, and d) relative humidity—for WRF-Var. The length scale controls the horizontal spread of the observations during the assimilation process.

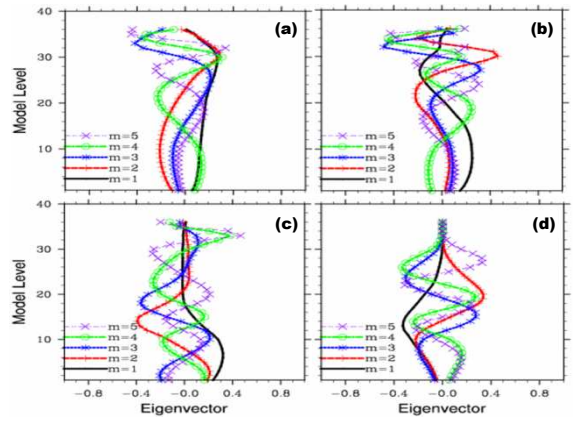

Fig. 4. Eigenvectors for each control variable—a) streamfunction, b) velocity potential, c) temperature, and d) relative humidity—for WRF-Var. Each color represents a mode of the eigenvectors with smaller modes controlling larger scales of vertical spread. The eigenvectors control the vertical spread of the observations during the assimilation process.

*3.3 The SPoRT **B** Matrix*

Correct use of the background error covariance matrix (**B** matrix) is important in determining the appropriate weighting between the background and observations, as well as how information contained in observations is spread horizontally and vertically. Optimal analysis configuration desires background errors that are consistent with the domain/grid spacing, the model used for the background, and the season. A SPoRT **B** was calculated using the National Meteorological Center (NMC) method of averaged forecast differences (Parrish and Derber 1992) using the "gen_be" program in the WRF-Var package. The differences between 24 and 12-h WRF forecasts for the 37-day case study period (17 January to 22 February 2007) were used to generate the **B** matrix. The background length scale and eigenvectors, which describe the horizontal and vertical spread of the observations, are shown in Figures 3 and 4 respectively. For both horizontal and vertical spread, lower vertical modes correspond to larger scales of spread. The average background error over the entire domain is shown back in Figure 2.

The SPoRT **B** provides a temperature and moisture length scale that is on the order of the analysis grid spacing. The first vertical mode, which analyzes large-scale features, is close to the grid spacing (Fig. 3c and d).

4. ANALYSIS IMPACT

The analysis impact of AIRS on 700 hPa temperature and mixing ratio for 17 January 2007 is shown in Figure 5. Figures 5a and 5b show the innovations of a Barnes analysis of the AIRS temperature and mixing ratio observations and the background field. AIRS temperatures are warmer across the southeast U.S. but are cooler across south Florida and the Great Lakes. The AIRS observations are at times 4°C warmer or cooler than the background. AIRS moisture is generally moister than the background, except in the region from the Florida panhandle to coastal South Carolina.

Figures 5c and 5d show the temperature and mixing ratio analysis increments for the AIRS analyses. The analysis increments depict ±2.5°C changes in a similar pattern to the innovations in Figure 5a—further emphasizing the impact of the AIRS observations on the analysis. The moisture fields at 700 hPa show a similar impact. The 700 hPa results are representative of results at most other levels.

To further illustrate the positive impact of the AIRS profiles, Figure 6 shows a comparison between a series of 0800 UTC soundings collocated near the Greensboro, NC (GSO) radiosonde site. The 0800 UTC radiosonde (green) is a linear interpolation of 0000 and 1200 UTC soundings. The background field (black) is too cool and dry below 600 hPa compared to the radiosonde. The AIRS observation (blue) at 0800 UTC is warmer and much moister than the background. As anticipated, when AIRS observations are assimilated, the analysis (red) becomes warmer and moister. For the temperature analysis, the inclusion of AIRS

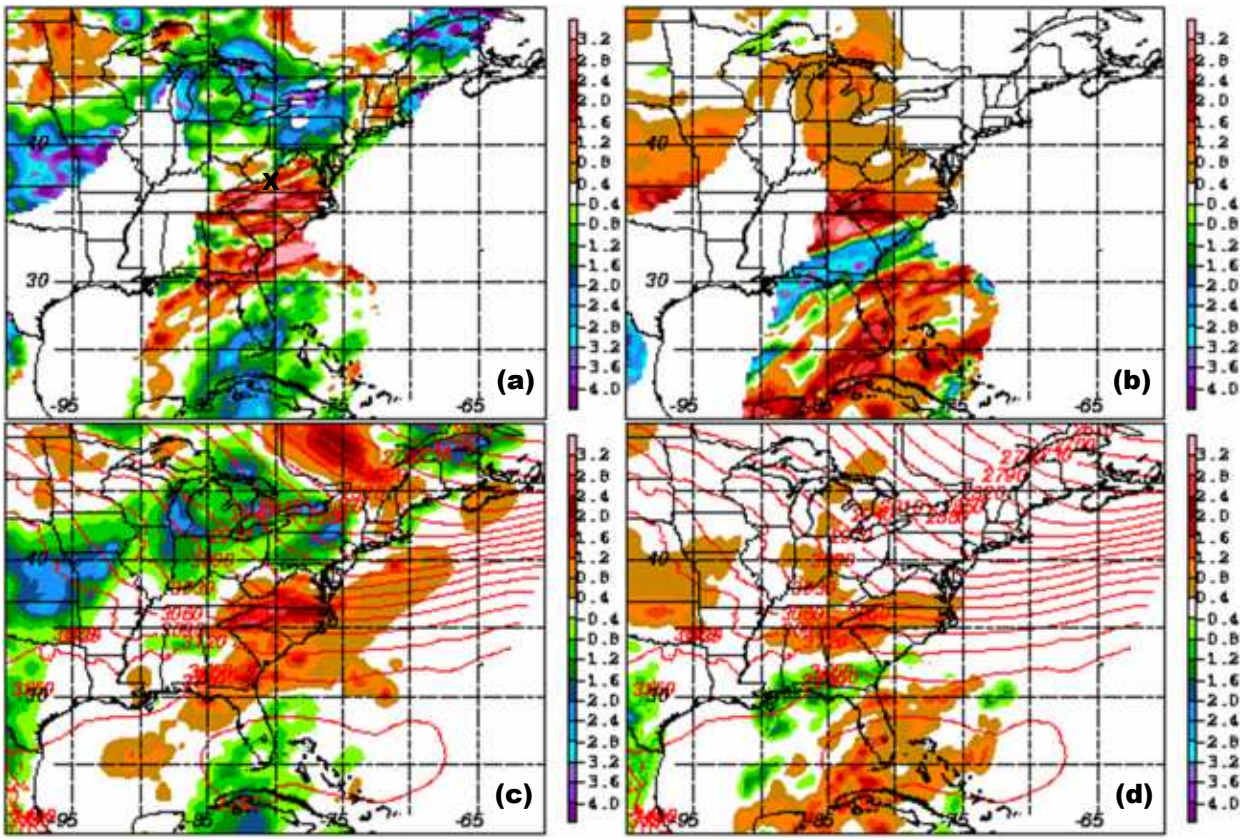

Fig. 5. Analysis impact of AIRS at 700 hPa for 0800 UTC 17 January 2007. The top row shows Innovation fields (AIRS-background) for a) temperature (°C) and b) mixing ratio (g/kg). The corresponding analysis increments (WRF-Var minus background) are shown in c) and d). The "x" in a) denotes the location of the Greensboro, NC (GSO) sounding described in Figure 6.

produces a superior analysis to the background (compared to the radiosonde) below 600 hPa. The moisture analysis pulls the analysis in the correct direction at 700 hPa but moistens the analysis too much compared to the radiosonde.

5. FORECAST IMPACTS

The impact of the AIRS profiles on sensible parameters in the WRF forecasts is conducted by comparing parallel runs of the WRF: one with AIRS (AIRS) and one without (CNTL). Comparisons were made to 50 radiosondes east of 105°W, and statistics were compiled every 12 hours for the daily 48-h forecasts from 17 January through 22 February 2007. For precipitation, verification is done by comparing the model outputs with the 4-km NCEP Stage IV precipitation data. The 6-h cumulative precipitation data are mapped to the WRF model domain for direct grid comparison. For consistency with the radiosonde verification, only grid points that lie to the east of 105°W longitude are used.

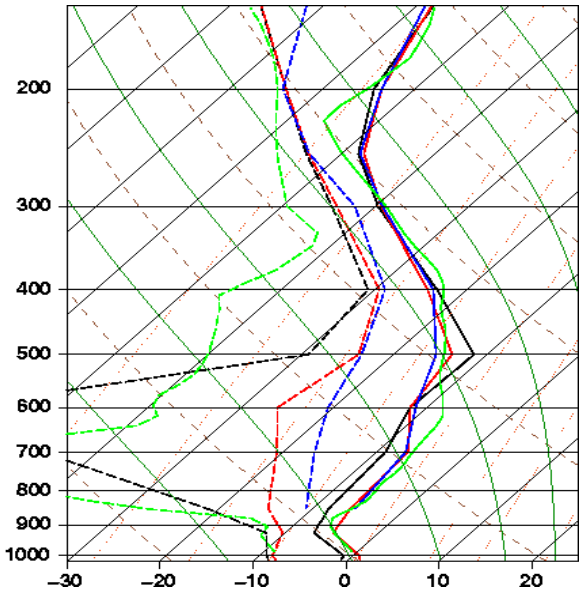

Fig. 6. Temperature (solid) and dew point (dashed) profiles near GSO for 0800 UTC 17 January 2007. The background (black) and WRF-Var (red) profiles are for the nearest grid point. The AIRS profile (blue) is for the highest-quality retrieval closest to the grid point. The radiosonde (green) is a linear interpolation to 0800 UTC.

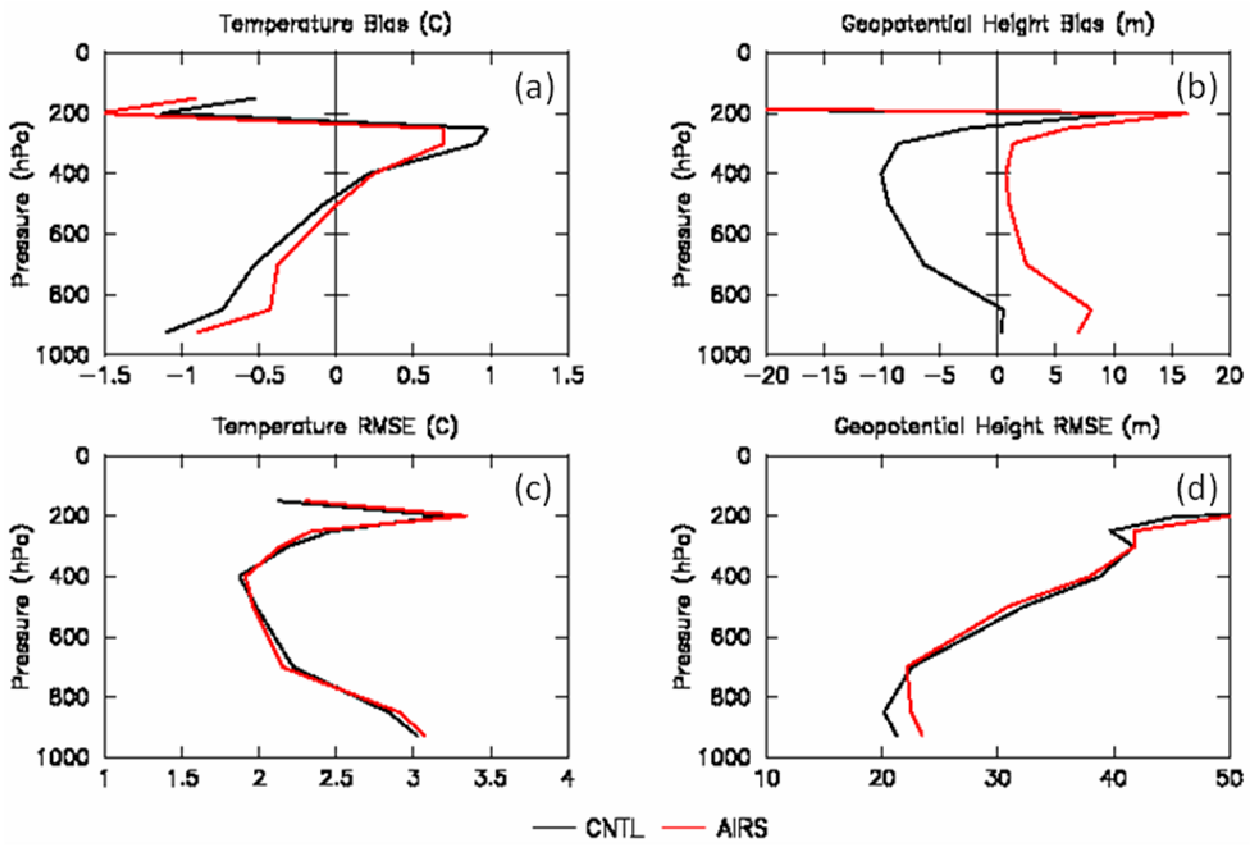

Fig. 7. Verification statistics of 48-h forecasts compared to 50 radisondes east of 105°W. Biases (forecast minus observations) for a) temperature (°C) and b) geopotential height (m) as well as root mean square error (RMSE) for c) temperature (°C) and d) geopotential height (m) for 37 days between 17 January and 22 February 2007 are shown. Black lines represent the CNTL cases; red lines represent the AIRS cases.

Figure 7 shows the cumulative statistics for the bias and root mean square error (RMSE) of temperature and geopotential height for all 37 48-h forecasts. Differences shown in Figure 7 are forecast minus observation such that biases less than zero indicate forecasts that have cooler temperatures and lower heights than the observations; biases greater than zero indicate forecasts that have warmer temperatures and higher heights.

For temperature, the CNTL run is cooler in the lower troposphere and warmer in the upper troposphere compared to the radiosondes. Most levels show a reduction in bias with the AIRS runs warming the cool-biased lower troposphere and cooling the warm-biased upper troposphere. The only noticeable RMSE difference between the AIRS and the CNTL is a slight decrease in RMSE between 700 and 500 hPa. To further investigate the results shown in Figure 7, a time series of the forecast bias at 700 hPa is shown in Figure 8a. In Figure 7, the AIRS forecasts are improved by approximately 0.2°C. Combining the improved RMSE in Figure 7c with the lack of a consistently warmer bias (i.e. some AIRS forecasts are cooler than the CNTL and some AIRS forecasts are warmer than the CNTL) leads to a conclusion of real forecasted temperature improvement with the inclusion of AIRS thermodynamic profiles.

The 48-h CNTL forecasts show geopotential heights that are too low compared to observations in the mid- to upper-troposphere. However, in the lower troposphere, the CNTL forecast is quite good. The AIRS profiles tend to raise the geopotential heights of the AIRS forecast throughout most of the troposphere, which works to reduce the bias in the mid- to upper troposphere (Fig. 7b). The height RMSE also shows slight improvement at the same levels. However, Figure 8 shows—via time series of 700 hPa heights—that the AIRS runs produce consistently higher heights. All but two forecasts show raised heights with the inclusion of AIRS profiles. This result combined with the result from Figure 7b leads to the conclusion that AIRS may be biasing the heights. This result may be due to changes in temperature not

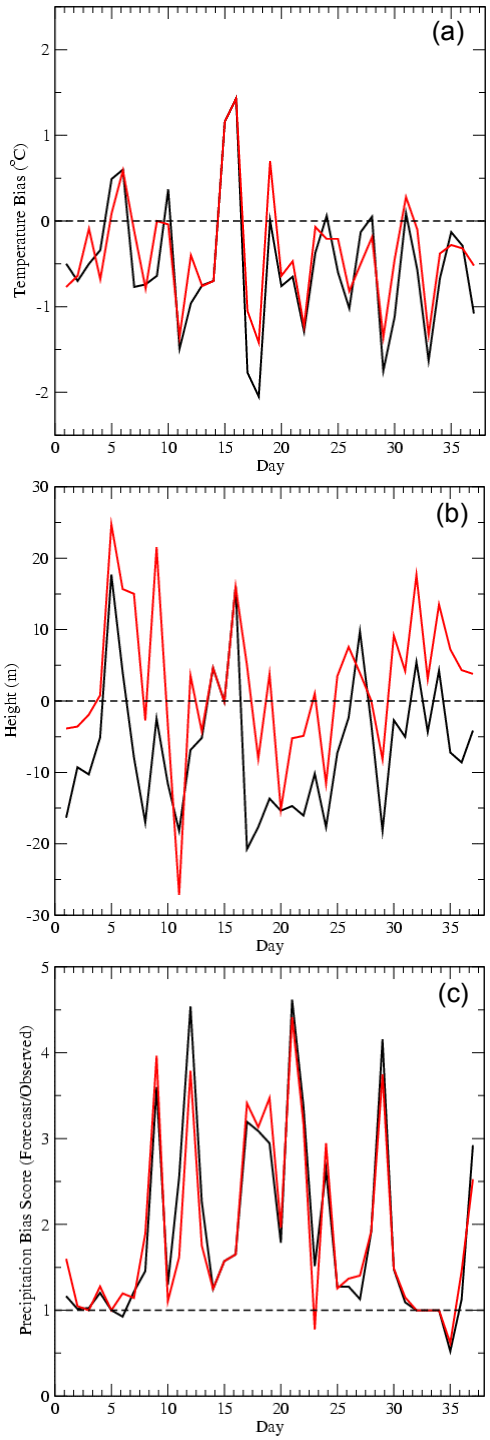

Fig. 8. Time series of each day in the 37-day case study period for 48-hr forecasts of a) 700 hPa temperature bias, b) 700 hPa geopotential height bias, and c) 6-hr cumulative precipitation bias score.

being appropriately balanced within the model and bias propagation throughout the forecast. This will be a point of further investigation.

Here, precipitation is verified using bias scores, which is equal to F/O, where F is the number of forecasted grid points that exceed any given precipitation threshold and O is the number of observed grid points that exceed that same threshold. Thus, the bias is a measure of the under- or over-forecasting of precipitation by the model. A bias score of 1 denotes perfect agreement in precipitation coverage between forecast and observations. Bias scores greater than 1 denote over forecasting; less than 1 denote under forecasting.

Overall, the average bias score for all measurable precipitation (greater than 2.54 mm) falling in 48-h forecasts for the 37 case study days is 1.48 for the CNTL runs and 1.51 for the AIRS runs. This means that AIRS slightly increases the precipitation in an already over-forecasted model. Figure 8c shows a time series of the 6-hr cumulative precipitation bias scores. For most days, the CNTL run over forecasts precipitation. Mostly, there are only small changes to the bias scores with the inclusion of AIRS observations. Further investigation into the dynamics of the precipitation development is necessary.

6. CONCLUSIONS

A methodology for assimilating v5.0 AIRS thermodynamic profiles into WRF-Var has been presented. A short-term WRF forecast was used as the background for the analysis, and quality indicators were used to select only the highest quality AIRS data, which were assimilated as separate land and water soundings. Results indicate that AIRS profiles produce an analysis closer to in situ observations than the background field, which should lead to improved initial conditions and better forecasts when used to initialize a model forecast. Forecasts from a 37-day case study period from the winter of 2007 were examined with mixed results. When compared against radiosonde observations, inclusion of AIRS thermodynamic profiles improved temperature bias, but produced consistently higher geopotential heights. Precipitation results are mixed for grid point comparisons with NCEP Stage IV precipitation data. More analysis of individual days from the case study is needed to better understand these results.

REFERENCES

Aumann, H. H., M. T. Chahine, C. Gautier, M. D. Goldberg, E. Kalnay, L. M. McMillin, H. Revercomb, P. W. Rosenkranz, W. L. Smith, D. H. Staelin, L. L. Strow, and J. Susskind, 2003: AIRS/AMSU/HSB on the Aqua Mission: Design, Science Objectives, Data Products, and Processing Systems. IEEE Transactions on Geoscience and Remote Sensing, 41, 253-264.

Barker, D. M., W. Huang, Y.-R. Guo, A. J. Bourgeois, and Q. N. Xiao, 2004: A Three-Dimensional Variational Data Assimilation System for MM5: Implementation and Initial Results. *Mon. Wea. Rev.*, **132**, 897-914.

Borbas, E. E., R. O. Knuteson, S. W. Seemann, E. Weisz, L. Moy, and H.-L. Huang, 2007: A high spectral resolution global land surface infrared emissivity database. *Preprints, 15th Satellite Meteorology and Oceanography Conference*, Amsterdam, The Netherlands, Amer. Meteor. Soc., P10.3

Chen, F. and J. Dudhia, 2001: Coupling an advanced land-surface/hydrology model with the Penn State/NCAR MM5 modeling system. Part I: Model description and implementation. Mon. Wea. Rev., 129, 569-585.

Duhdia, J., 1989: Numerical study of convection observed during the winter monsoon experiment using mesoscale two-dimensional model. *J. Atmos. Sci.*, **46**, 3077-3107.

Goodman, S. J., W. M. Lapenta, G. J. Jedlovec, J. C. Dodge, and T. Bradshaw, 2004: The NASA Short-term Prediction Research and Transition (SPoRT) Center: A collaborative model for accelerating research into operations. Preprints, *20th Conference on Interactive Information Processing Systems (IIPS)*, Seattle, WA, Amer. Meteor. Soc., P1.34.

Janjic, Z. I., 1990: The step-mountain coordinate: Physical package. *Mon. Wea. Rev.*, **118**, 1429-1443.

Kain, J. S., and J. M. Fritsch, 1990: A one-dimensional entraining/detraining plume model and its application in convective parameterization. *J. Atmos. Sci.*, **49**, 2784-1802.

Le Marshall, J., J. Jung, J. Derber, M. Chahine, R. Treadon, S. J. Lord, M. Goldberg, W. Wolf, H. C. Liu, J. Joiner, J. Woollen, R. Todling, P. van Delst, and Y. Tahara, 2006: Improving Global Analysis and Forecasting with AIRS. *Bull. Amer. Met. Soc.*, 87, 891-894.

Mellor, G. L., and T. Yamada, 1982: Development of a turbulence closure model for geophysical fluid problems. *Rev. Geophys. And Space Phys.*, **20**, 851-875.

Mlawer, E. J., S. J. Taubman, P. D. Brown, M. J. Iacono, and S. A. Clough, 1997: Radiative transfer for inhomogeneous atmosphere: RRTM, a validated correlated-k model for the long-wave. *J. Geophys. Res.,* **102 (D14)**, 16663-16682.

Susskind, J., C. Barnet, J. Blaisdell, L. Irdell, F. Keita, L. Kouvaris, G. Molnar, and M. Chahine, 2006: Accuracy of geophysical parameters derived from Atmospheric Infrared Sounder/Advanced Microwave Sounding Unit as a function of fractional cloud cover, *J. Geophys. Res.*, **111**, D09S17, 19 pp.

Tobin, D. C., H. E. Revercomb, R. O. Knuteson, B. M. Lesht, L. L. Strow, S. E. Hannon, W. F. Feltz, L. A. Moy, E. J. Fetzer, and T. S. Cress, 2006: ARM site atmospheric state best estimates for AIRS temperature and water vapor retrieval validation. *J. Geophys. Res.*, **111**, D09S14, 18 pp.